

# QSAN: A Near-term Achievable Quantum Self-Attention Network

Ren-xin Zhao<sup>1</sup>, Jinjing Shi<sup>1</sup>, Shichao Zhang<sup>1</sup>

<sup>1</sup> School of Computer Science and Engineering, Central South University, Changsha, China

**Abstract**—Self-attention mechanism, an important component of machine learning, has been relatively little investigated in the field of quantum machine learning. Inspired by the variational Quantum Algorithm (VQA) framework and classical self-attention mechanism, Quantum Self-Attention Network (QSAN) that can be implemented on a near-term quantum computer is proposed. Theoretically, Quantum Self-Attention Mechanism (QSAM) is defined, which is a new interpretation of the classical self-attention mechanism after linearization and logicalization. Quantum Logical Similarity (QLS) is one of the cores of QSAM, which replaces the similarity operation of inner product with logical operation, allowing a better execution of QSAM on quantum computers. Quantum Bit Self-Attention Score Matrix (QBSASM) is another centerpiece, which is a QLS-based density matrix used to represent the output distribution. In practice, QSAN is realized based on the QSAM framework, and the concept of quantum coordinates is introduced to simplify circuit design. Finally, QSAN is tested on a quantum computer with a small sample of data, laying the foundation for Quantum Natural Language Processing (QNLP).

**Index Terms**—Quantum Self Attention Mechanism, Quantum Circuit, Quantum Natural Language Processing, Quantum Machine Learning, Quantum Network.

## I. INTRODUCTION

Self-attention mechanism is a powerful component embedded in the machine learning framework. It is originally introduced for machine translation [1], and now is extensively employed in Natural Language Processing (NLP) [2], Speech [3], and Computer Vision [4].

Self-attention mechanism reduces the reliance on external information and is more skilled at capturing the internal relevance of data or features, which significantly improves the performance of the model in NLP tasks. Theoretically, the space and time complexity of the self-attentive mechanism are both  $O(n^2)$ , where  $n$  is the sequence length. Therefore, optimizing the self-attentive mechanism becomes a meaningful task. Ref. [5] took the idea of sparsification. The core concept is to diminish the computational effort of the binding law, i.e., to consider each element to be related to only a part of the sequence. Ref. [6] suggested a linearization scheme, which splits the dot product softmax into the dot product of two softmaxes, making its storage efficiency and computational efficiency twice as high as that of the dot product attention mechanism. Besides, linearization schemes such as random

Ren-xin Zhao and Jinjing Shi is with School of Computer Science and Engineering, Shaoshan South Road, Tianxin District, Changsha City, Hunan Province, China. (e-mail:13061508@alu.hdu.edu.cn; shijinjing@csu.edu.cn)

Corresponding author: Jinjing Shi.

projection [7], Nyström's method [8] and gated attention units [9] have been introduced one after another.

The above optimizations of the self-attention mechanism are based on classical computers. Quantum computer is considered as a new processor paradigm to break the arithmetic limit of classical computers and has made a great breakthrough in recent years [10–12]. The advantage possessed by quantum computers, also called quantum supremacy, i.e. an advantage that is difficult to simulate by classical computers, can be understood superficially as the exponential storage and exponential computational acceleration of quantum computers due to their quantum properties [13, 14]. The development of quantum computers has given rise to new fields such as QNLP. QNLP is generally recognized as having a secondary acceleration effect over NLP. Recent work in QNLP mainly comes from [15, 16], which have augmented classical machine learning models by replacing classical neural network layers with Parametric Quantum Circuits (PQC) built on NISQ [17] devices using VQA [18–28]. Nevertheless, none of the above proposals has explored quantum solutions for attention mechanisms.

Inspired by [1, 18], QSAN, a quantum network version of the self-attention mechanism, is proposed. QSAN is a quantum circuit with a process similar to [1] but with probabilistic properties, parallel computational characteristics, and can be embedded in classical or quantum machine learning models. In particular, the dimensionality of the QBSASM generated by QSAN shows an exponential growth, which is difficult to simulate on a normal computer. Around QSAN, the contributions in this paper are as follows:

- ★ The QSAM theoretical framework is constructed, which is a linearized and logical version of the classical self-attention mechanism that is more easily deployed on quantum computers.
- ★ Two core ideas are proposed: QLS and QBSASM. QLS uses logical operations instead of inner product operations to ensure that QSAM can be executed more thoroughly on quantum computers; QBSASM is a density matrix based on QLS to measure the output distribution.
- ★ Based on the above theory, the modules of QSAN are constructed to obtain the output word vectors and QBSASM at once, while being easy to implement under the idea of quantum coordinates.

This article is organized as follows. Some basics are reviewed in Section II. Section III introduces QLS, QBSASM, and QSAM, which serve as the theoretical basis for the birth of

QSAN. The potential of quantum coordinates and the design of QSAN are presented in Section IV. Section V shows the results of small sample tests of QSAN in IBM qiskit and pennylane environments, as well as makes some useful discussions.

## II. PRELIMINARIES

This section briefly overview the classical attention mechanism, VQA and quantum operators. First of all, it should be noted here that subscripts always signify the variable's serial number if not otherwise specified in the text.

### A. Self Attention

Suppose there is an input vocabulary set  $\mathbf{In} = \{\mathbf{w}_0, \dots, \mathbf{w}_{n-1}\}$  and an output set  $\mathbf{Out} = \{\mathbf{new\_w}_0, \dots, \mathbf{new\_w}_{n-1}\}$ , where each element  $\mathbf{w}_i, \mathbf{new\_w}_j, i, j \in \{0, \dots, n-1\}$  and  $\mathbf{Out}$  is a vector of dimension  $l$ . And  $n$  is the number of word vectors. Then the classical self-attention mechanism [1] can be stated as

$$\mathbf{new\_w}_i = \sum_j \text{softmax} \left( \frac{\mathbf{Q}_i \mathbf{K}_j^T}{\sqrt{d}} \right) \mathbf{V}_j. \quad (1)$$

In Eq. (1),  $\mathbf{Q}_i, \mathbf{V}_j$  are row vectors, where

$$\mathbf{Q}_i = \mathbf{U}_Q \cdot \mathbf{w}_i$$

and

$$\mathbf{V}_j = \mathbf{U}_V \cdot \mathbf{w}_j$$

represents new word vector after the weighting operation. The weights are also known as attention score and are obtained by normalizing the inner product  $\mathbf{Q}_i \mathbf{K}_j^T$  in Eq. (1).  $\mathbf{K}_j^T$  is a column vector, which is the transpose of

$$\mathbf{K}_j = \mathbf{U}_K \cdot \mathbf{w}_j$$

$\mathbf{U}_Q, \mathbf{U}_K, \mathbf{U}_V$  are named as query matrix, key-value matrix and value matrix respectively and they are three trainable parameter matrices.

### B. VQA

In the NISQ era, it is very difficult to fully deploy deep networks for deep learning on quantum computers with limited quantum bits. On the one hand, the dimensionality of the model grows exponentially as the size of the quantum circuit gets larger and larger [19]. On the other hand, noise imposes many unknowns on the training results [20]. Therefore, quantum-classical hybrid models can be deemed as an efficient path. VQA is one such class of algorithms. Fig. 1 exhibits the framework of VQA, which can be divided into two parts.

1. The pink box designates the range of the classical computer. This stage focuses on the calculation of the loss function and the optimization of the parameters, as shown in the two purple curves in Fig. 1. The general formulation of the loss function is:

$$C(\theta) = \sum_k f_k(\text{Tr}[O_k \mathbf{U}(\theta)] \rho_k \mathbf{U}^\dagger(\theta)) \quad (2)$$

where  $f_k$  is a set of certain functions determined by specific tasks.  $\mathbf{U}(\theta) = \otimes_i U_i(\theta_i)$  denotes the product of a series of

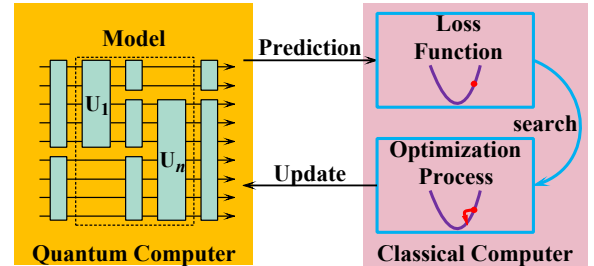


Fig. 1: Framework of VQA

unitary operators, where  $\theta$  comprises a series of continuous or discrete hyperparameters.  $\{\rho_k\}$  is the input state of the training set, and  $O_k$  is a set of observables. Some strategies for training loss functions can be consulted in [21–23].

2. The tan box stands for the quantum computer domain. In this box, a PQC model is drawn. The black dashed box is the centerpiece of this model, the Ansatz, which is a circuit with a specific structure and function. Common examples of Ansatz contain hardware-efficient Ansatz (a quantum circuit model that decreases the circuit depth required to implement  $\mathbf{U}(\theta)$  for a given quantum hardware) [24, 25], quantum alternating operator Ansatz (can searches for optimal solutions to combinatorial optimization problems) [26–28], etc.

The arrows in the figure illustrate the interaction of information between a quantum computer and a classical computer. The quantum computer provides the classical computer with quantum circuit measurements and loss function forms to be used for prediction. After the classical computer is trained, a new round of hyperparameters is uploaded and updated into the quantum circuit.

### C. Qubit and Operators

The smallest unit of information in a quantum computer is a qubit  $|\psi\rangle$  which can be represented as a linear superposition of two eigenstates  $|0\rangle$  and  $|1\rangle$ , namely

$$|\psi\rangle = \alpha|0\rangle + \beta|1\rangle$$

where  $\alpha$  and  $\beta$  are probability amplitudes and satisfy

$$|\alpha|^2 + |\beta|^2 = 1.$$

These qubits evolve through unitary operators  $U$  which are also called quantum gates and refer to matrices that satisfy

$$U = U^\dagger$$

$$UU^\dagger = \mathbb{I}$$

where  $U^\dagger$  is the complex conjugate of  $U$ . This article mainly uses Pauli Y Gate

$$Y = \begin{pmatrix} 0 & -i \\ i & 0 \end{pmatrix},$$

Hadamard Gate

$$H = \frac{1}{\sqrt{2}} \begin{pmatrix} 1 & 1 \\ 1 & -1 \end{pmatrix},$$

SWAP gate

$$\text{SWAP} = \begin{pmatrix} 1 & 0 & 0 & 0 \\ 0 & 0 & 1 & 0 \\ 0 & 1 & 0 & 0 \\ 0 & 0 & 0 & 1 \end{pmatrix},$$

CNOT gate

$$CNOT = \begin{pmatrix} 1 & 0 & 0 & 0 \\ 0 & 1 & 0 & 0 \\ 0 & 0 & 0 & 1 \\ 0 & 0 & 1 & 0 \end{pmatrix},$$

and Toffoli gate

$$Toffoli = \begin{pmatrix} 1 & 0 & 0 & 0 & 0 & 0 & 0 & 0 \\ 0 & 1 & 0 & 0 & 0 & 0 & 0 & 0 \\ 0 & 0 & 1 & 0 & 0 & 0 & 0 & 0 \\ 0 & 0 & 0 & 0 & 0 & 0 & 0 & 1 \\ 0 & 0 & 0 & 0 & 1 & 0 & 0 & 0 \\ 0 & 0 & 0 & 0 & 0 & 1 & 0 & 0 \\ 0 & 0 & 0 & 0 & 0 & 0 & 1 & 0 \\ 0 & 0 & 0 & 1 & 0 & 0 & 0 & 0 \end{pmatrix}.$$

### III. QUANTUM SELF-ATTENTION MECHANISM

This section will focus on the QSAM framework. In this framework, QLS is a custom logical similarity. It makes QSAM free from building complex networks of quantum numerical operations, saves qubits, and is easier to accomplish on quantum computers. And QBSASM is a special density matrix based on QLS. It is used to express the distribution of the output and each element of it is calculated by QLS.

Before starting, first the sets **In** and **Out** are re-expressed in quantum states as  $\mathbf{Q}_{\text{in}} = \{|\mathbf{w}_0\rangle, \dots, |\mathbf{w}_{n-1}\rangle\}$  and  $\mathbf{Q}_{\text{out}} = \{|\mathbf{new\_w}_0\rangle, \dots, |\mathbf{new\_w}_{n-1}\rangle\}$  respectively, where each element  $|\mathbf{w}_a\rangle, a \in \{0, \dots, n-1\}$  of  $\mathbf{Q}_{\text{in}}$  is a vector of dimension  $m = \lceil \log_2 l \rceil$ , and  $l$  is the feature dimension of the classical word vector. The dimension of  $|\mathbf{new\_w}_b\rangle, b \in \{0, \dots, n-1\}$  is higher, mainly because QSAM is described as

$$|\mathbf{new\_w}_i\rangle = \bigoplus_j \langle \mathbf{Q}_i | \mathbf{K}_j \rangle \otimes |\mathbf{V}_j\rangle. \quad (3)$$

In Eq. (3),

$$\begin{aligned} |\mathbf{Q}_i\rangle &= U_q |\mathbf{W}_i\rangle, \\ |\mathbf{K}_j\rangle &= U_k |\mathbf{W}_j\rangle, \\ |\mathbf{V}_j\rangle &= U_v |\mathbf{W}_j\rangle \end{aligned}$$

where  $U_q$ ,  $U_k$  and  $U_v$  are three composite unitary operators with the identical structure but distinct parameters. Each of them is composed of a number of Hadamard gates, Pauli Y gates and CNOT gates, that is,

$$U_{M \in \{q, k, v\}} = CNOT^{\otimes(m-1)} R_y(\theta_M)^{\otimes m} H^{\otimes m}. \quad (4)$$

The benefit of this structure is that it ensures that the probability amplitudes are real [33].  $|\mathbf{w}_i\rangle$  and  $|\mathbf{w}_j\rangle$  are input word vectors. Furthermore, the symbol  $\oplus$  represents a modulo-two addition,  $\langle \mathbf{Q}_i | \mathbf{K}_j \rangle$  is QLS that will be introduced next.

Formally, Eq. (3) is very similar to Eq. (1), but there are significant distinctions. The most essential difference is that Eq. (1) is a nonlinear attention mechanism due to the softmax function in the formula, while the linear attention mechanism proposed in this paper is a linear attention mechanism that can be solved by quantum circuits. In addition, by the modification, Eq. (3) avoids the numerical operations such as addition in Eq. (1), which eliminates the need to build a larger network of quantum numerical operations, thus saving qubits.

#### A. Quantum Logical Similarity

In quantum computing, a common way to characterize the similarity between two quantum states  $|\mathbf{Q}_a\rangle$  and  $|\mathbf{K}_b\rangle$  is SWAP test [29] or Hadamard test [30]. However, these two schemes are made by multiple measurements to obtain the inner product of quantum states. Yet, the goal of QSAM is not to obtain the similarity between quantum states, but to construct new word vectors with the help of similarity. Therefore, the classical method of using inner product as similarity must be modified.

**Definition 1** (QLS): For any quantum state  $|\mathbf{Q}_a\rangle, |\mathbf{K}_b\rangle, a, b \in \{0, \dots, n-1\}$ , then

$$\langle \mathbf{Q}_a | \mathbf{K}_b \rangle = \bigoplus_j (qb_j \wedge kb_j) \quad (5)$$

where  $|qb_j\rangle$  and  $|kb_j\rangle$ ,  $j \in \{0, \dots, m-1\}$  denote the  $j$ -th qubit of  $|\mathbf{Q}_a\rangle$  and  $|\mathbf{K}_b\rangle$ , respectively. The symbol  $\oplus$  indicates modulo-two addition and the symbol  $\wedge$  is logical AND operation. Eq. (5) may seem counter-intuitive, but in fact, an AND operation can be performed between two superposition states, and the consequence is also a superposition state. From the implementation point of view, AND operation and modulo-two addition can be realized with Toffoli gates and CNOT gates, respectively. Eq. (5) is then explained in terms of quantum gates:

$$\begin{aligned} &Toffoli|qb_j^a, kb_j^b, 0\rangle \\ &= |qb_j^a, kb_j^b, qb_j^a \wedge kb_j^b\rangle \\ &CNOT|qb_j^a \wedge kb_j^b, qb_j^a \wedge kb_j^b\rangle \\ &= |qb_j^a \wedge kb_j^b, (qb_j^a \wedge kb_j^b) \oplus (qb_j^a \wedge kb_j^b)\rangle. \end{aligned}$$

Moreover, Eq. (5) is obviously consistent with the commutation law, i.e.

$$\langle \mathbf{Q}_a | \mathbf{K}_b \rangle = \langle \mathbf{K}_b | \mathbf{Q}_a \rangle,$$

which contributes to computational efficiency and avoidance of barren plateaus due to heavy entanglement [31, 32]. This property states that Eq. (5) only needs to calculate  $m \sum_{i=1}^n i$  times instead of  $n^2$  times.

#### B. Quantum Bit Self-Attention Score Matrix

Eq. (3) gives the procedure for solving the quantum circuit for a single new word vector only. The process of solving for all word vectors is re-described using matrices. The specific formula is as follows:

$$\begin{aligned} &\begin{pmatrix} \langle \mathbf{Q}_0 | \mathbf{K}_0 \rangle & \langle \mathbf{Q}_0 | \mathbf{K}_1 \rangle & \cdots & \langle \mathbf{Q}_0 | \mathbf{K}_{n-1} \rangle \\ \langle \mathbf{Q}_1 | \mathbf{K}_0 \rangle & \langle \mathbf{Q}_1 | \mathbf{K}_1 \rangle & \cdots & \langle \mathbf{Q}_1 | \mathbf{K}_{n-1} \rangle \\ \vdots & & & \vdots \\ \langle \mathbf{Q}_{n-1} | \mathbf{K}_0 \rangle & \cdots & \cdots & \langle \mathbf{Q}_{n-1} | \mathbf{K}_{n-1} \rangle \end{pmatrix} \begin{pmatrix} |\mathbf{V}_0\rangle \\ |\mathbf{V}_1\rangle \\ \vdots \\ |\mathbf{V}_{n-1}\rangle \end{pmatrix} \\ &= \begin{pmatrix} |\mathbf{new\_word}_0\rangle \\ |\mathbf{new\_word}_1\rangle \\ \vdots \\ |\mathbf{new\_word}_{n-1}\rangle \end{pmatrix} \end{aligned} \quad (6)$$

where

$$\begin{pmatrix} \langle \mathbf{Q}_0 | \mathbf{K}_0 \rangle & \langle \mathbf{Q}_0 | \mathbf{K}_1 \rangle & \cdots & \langle \mathbf{Q}_0 | \mathbf{K}_{n-1} \rangle \\ \langle \mathbf{Q}_1 | \mathbf{K}_0 \rangle & \langle \mathbf{Q}_1 | \mathbf{K}_1 \rangle & \cdots & \langle \mathbf{Q}_1 | \mathbf{K}_{n-1} \rangle \\ \vdots & & & \vdots \\ \langle \mathbf{Q}_{n-1} | \mathbf{K}_0 \rangle & \cdots & \cdots & \langle \mathbf{Q}_{n-1} | \mathbf{K}_{n-1} \rangle \end{pmatrix} \quad (7)$$

is called QBSASM, which is a square matrix with each element consisting of a different QLS  $\langle \mathbf{Q}_i | \mathbf{K}_j \rangle$ . The QBSASM can be analyzed by intercepting the density matrix.

In summary, the output  $\langle \mathbf{Q}_a | \mathbf{K}_b \rangle$  is the superposition state of a single qubit. Because of this, the dimensionality of QBSASM is much higher than the classical attention score matrix, because each element of it is not a scalar but a qubit. Finally, it can be known that the output of Eq. (3) are 1 more than the input. But there is no need to worry about the different dimensions of the input and output, using a layer of neural network can effectively control the output dimensionality.

#### IV. QUANTUM SELF-ATTENTION NETWORK

In this section, QSAN is constructed under the theoretical framework of the previous section, following a process similar to that of Ref. [1]. This network can obtain word vector outputs as well as QBSASM in a single step.

The main framework of QSAN, as shown in Fig. 2, consists of four registers, one input register and three garbage registers for computing  $|\mathbf{Q}\rangle = \otimes_{t=0}^{n-1} |\mathbf{Q}_t\rangle$ ,  $|\mathbf{K}\rangle = \otimes_{t=0}^{n-1} |\mathbf{K}_t\rangle$  and  $\langle \mathbf{Q} | \mathbf{K} \rangle$ . Among these registers, the first, second and third registers require  $n \times m$  quantum bits, respectively. The fourth register requires  $m \sum_{i=1}^n i$  qubits. In total,  $3m \times n + m \sum_{i=1}^n i$  qubits are needed. Another thing to pay attention to is the initialization state of each register. Here it is specified that the first three registers in Fig. 2 have the same initial value. This step can be implemented in code. The input here is denoted as  $|\mathbf{In}\rangle = \otimes_{t=0}^{n-1} |\mathbf{W}_t\rangle$ , and the output through  $U_v$  is denoted as  $|\mathbf{V}\rangle = \otimes_{t=0}^{n-1} |\mathbf{V}_t\rangle$ . Then start the step-by-step anatomy of QSAN, and explain its details.

Step 1: Calculate  $|\mathbf{Q}\rangle$ , that is

$$|U_q^{\otimes n} \mathbf{In}, \mathbf{In}, \mathbf{In}, \mathbf{0}\rangle = |\mathbf{Q}, \mathbf{In}, \mathbf{In}, \mathbf{0}\rangle,$$

where  $U_q^{\otimes n}$  as shown in Fig. 3 represents applying the gate circuit as in Eq. (4) to each word vector.

From Fig. 3, it can be seen that each word vector is applied with  $m$  Hadamard gates,  $m$  Pauli Y gates, and  $m-1$  CNOT gates. But for a more macro analysis, it is necessary to define a concept of coordinates.

**Definition 2** (gate coordinates): For a quantum network in which quantum gates are regularly distributed, the line numbers of the registers where the control/input bits or output bits of these gates are located are defined as the coordinates of the quantum gates.

Among these control coordinates as well as output coordinates, the output coordinates tend to be more concerned because it serves as the input of the next layer. The introduction of gate coordinates can simplify programming and enhance the interpretability of quantum networks. In addition, its effect on line simplification is also worthy of study.

Here, a CNOT gate coordinate law between words that is generally applicable to this project is proposed. In the same register

$$CNOT[s(t), s(t) + 1] \quad (8)$$

where

$$s(t) = m \times \frac{t - t \bmod (m-1)}{m-1} + t \bmod (m-1) \quad (9)$$

is a general term formula with respect to  $t$ . This expression is more concise. The logical function it implies is to XOR the  $s(t)$ -th and  $s(t) + 1$ -th in the same register. The value range of  $t$  depends on the situation.

Step 2: Temporarily store  $|\mathbf{Q}\rangle$ , and reset the input

$$SWAP^{\otimes(m \times n)} |\mathbf{Q}, \mathbf{In}, \mathbf{In}, \mathbf{0}\rangle = |\mathbf{In}, \mathbf{Q}, \mathbf{In}, \mathbf{0}\rangle$$

where  $SWAP^{\otimes(m \times n)}$  as shown in Fig. 4 indicates that the SWAP gate must be used for each dimension of each word vector.

Step 3: Calculate  $|\mathbf{K}\rangle$ ,

$$|U_k^{\otimes n} \mathbf{In}, \mathbf{Q}, \mathbf{In}, \mathbf{0}\rangle = |\mathbf{K}, \mathbf{Q}, \mathbf{In}, \mathbf{0}\rangle.$$

Step 4: Temporarily store  $|\mathbf{K}\rangle$ , and reset the input

$$SWAP^{\otimes(m \times n)} |\mathbf{K}, \mathbf{Q}, \mathbf{In}, \mathbf{0}\rangle = |\mathbf{In}, \mathbf{Q}, \mathbf{K}, \mathbf{0}\rangle.$$

Step 5: Calculate  $\langle \mathbf{Q} | \mathbf{K} \rangle$  according to Eq. (5) as shown in Fig. 5

$$Toffoli^{\otimes(m \sum_{i=1}^n i)} |\mathbf{In}, \mathbf{Q}, \mathbf{K}, \mathbf{0}\rangle = |\mathbf{In}, \mathbf{Q}, \mathbf{K}, \mathbf{Q} \wedge \mathbf{K}\rangle$$

where

$$\mathbf{Q} \wedge \mathbf{K} = \otimes_{t,j} Toffoli[p_1, p_2, p_3(t, j)] \quad (10)$$

where  $p_1 = t + m \times n, p_2 = t + 2m \times n, p_3(t, j) = t + m \times j + m(\sum_{c=1}^{n-1} c - \sum_{d=1}^{n-1} \lfloor t/m \rfloor d) + 3m \times n, t \in \{0, \dots, m \times n - 1\}, j \in \{0, \dots, n - \lfloor t/m \rfloor - 1\}$

Eq. (10) uses the idea of coordinates again. The expression means that the  $p_1$ -th qubit located in the second garbage register is ANDed with the  $p_2$ -th qubit located in the third garbage register, and the result is stored in the  $p_3$ -th qubit of the fourth register.

The CNOT gates are then applied to the fourth garbage register

$$\langle \mathbf{Q} | \mathbf{K} \rangle = \otimes_t CNOT[s(t) + 3m \times n, s(t) + 3m \times n + 1]$$

where  $t \in \{0, \dots, (m-1) \sum_{i=1}^n i\}$ . Among all the outputs  $s(t) + 1$ ,

$$g(o) = m \times o - 1 |_{o \in \{1, \dots, \sum_{i=1}^n i\}} \quad (11)$$

is really desired according to Eq. (5), which stands for the true output of Eq. (8).

From this step, it is found that the attention coefficient matrix is equivalent to the density matrix expression after  $\langle \mathbf{Q} | \mathbf{K} \rangle$  measurement, and the corresponding attention matrix can be drawn with IBM qiskit.

Step 6: Calculate  $|\mathbf{V}\rangle$ , and get the final Eq. (3) as shown in Fig. 6

$$|U_v^{\otimes n} \mathbf{In}, \mathbf{Q}, \mathbf{K}, \langle \mathbf{Q} | \mathbf{K} \rangle\rangle = |\mathbf{V}, \mathbf{Q}, \mathbf{K}, \langle \mathbf{Q} | \mathbf{K} \rangle\rangle$$

CNOT gates are added again for  $|\mathbf{V}\rangle$  and  $\langle \mathbf{Q} | \mathbf{K} \rangle$ . The specific way of adding CNOT is executed according to Eq. (6). Specifically,

$$CNOT^{\otimes(m \times n)} |\mathbf{V}\rangle = \bigotimes_{i=0}^{m-1} \bigoplus_{j=0}^{n-1} v b_{i+m \times j}^j \quad (12)$$

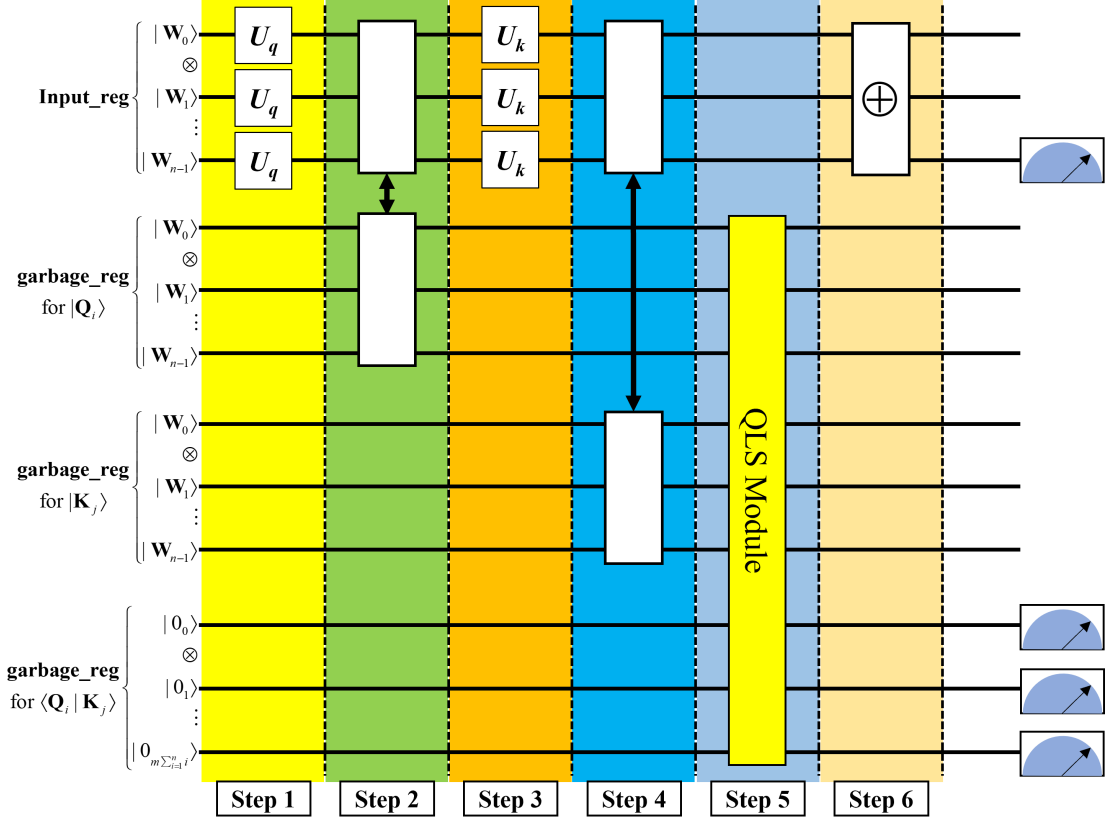
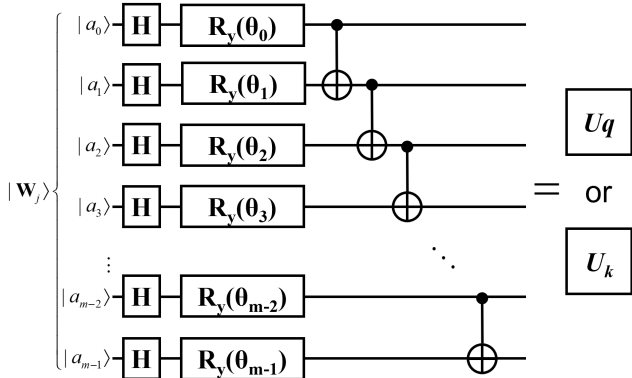


Fig. 2: Circuit Model of QSAN

Fig. 3: Circuit for  $U_q$  or  $U_k$ 

if  $|\mathbf{V}_i\rangle$  is written as

$$|\mathbf{V}_i\rangle = \begin{pmatrix} |vk_0^i\rangle \\ \vdots \\ |vk_{m-1}^i\rangle \end{pmatrix}$$

where  $|vk_j^i\rangle$  indicates the  $j$ -th quantum bit of the  $i$ -th word vector. Then apply a CNOT gate to the elements of each row of Eq. (7) as well,

$$\bigotimes_{j_1=0}^{n-1} \bigoplus_{j_2=0}^{n-1} \langle \mathbf{Q}_{j_1} | \mathbf{K}_{j_2} \rangle \quad (13)$$

where  $j_1$  is the row number and  $j_2$  is the column number. Observing Eq. (7), Eq. (13) and Eq. (11), it is found that the

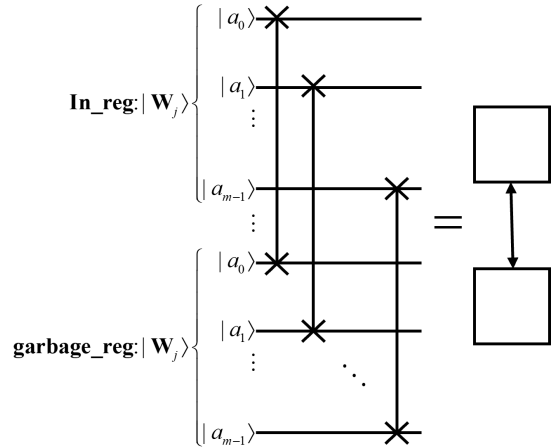


Fig. 4: Circuit for SWAP

weight matrix is a symmetric matrix and has the following relationship with the parameter  $o$  of Eq. (11):

$$o = \begin{cases} 1 + \sum_{i=1}^n i - \sum_{j=1}^{n-\text{row}} j + \text{col} & \text{row} \leq \text{col} \\ \text{row}_1 + 1 + \sum_{i=1}^{n-1} i - \sum_{j=1}^{n-1-\text{col}_1} j & \text{row}_1 > \text{col}_1 \end{cases} \quad (14)$$

where  $\text{row} \in \{0, \dots, n-1\}$ ,  $\text{col} \in \{0, \dots, n-\text{row}\}$ ,  $\text{row}_1 \in \{1, \dots, n-1\}$ ,  $\text{col}_1 \in \{0, \dots, \text{row}_1\}$ .

Here the equivalence between the coordinates of the quan-

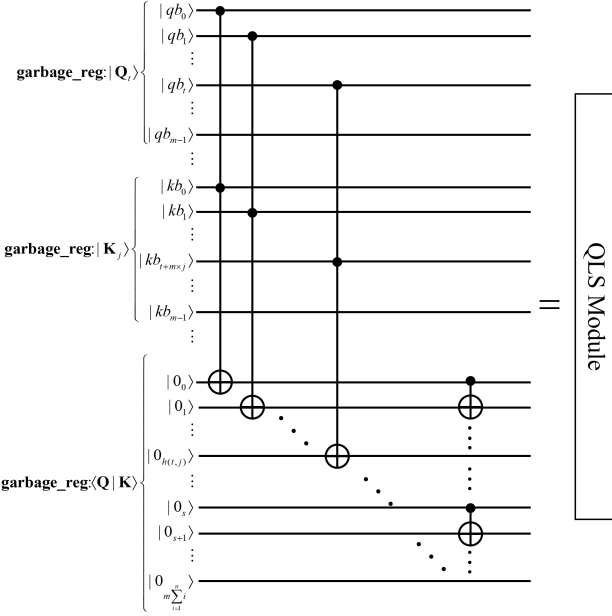
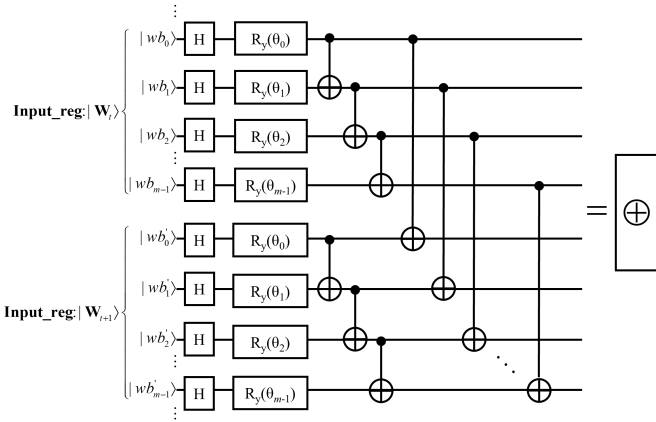


Fig. 5: Circuit for QLS module

Fig. 6: Circuit for  $CNOT^{(m \times n)} |V\rangle$ 

tum gate and the positions of the elements of the weight matrix is established, then the coordinates of the quantum gate can be confirmed by retrieving the positions of the corresponding elements.

Step 7: Combined measurements. This step is measured with skill. Choosing the full output qubit of Eq. (12) and one of the qubits in Eq. (13), the corresponding word vector can be formed, which also conforms to the reality that the output has 1 more dimension than the input. If the dimensionality is to be guaranteed to be the same, a layer of neural network can be used.

## V. EXPERIMENT AND DISCUSSION

This subsection implements the simulation of QSAN using IBM Qiskit and pennylane.

**Preparation** Currently quantum bits are severely limited, so an attempt is made to verify the feasibility of this scheme with a small homemade data sample. Firstly, two classical word vectors follow Transformer's practice and form a new

set of samples by positional encoding [1]. Each new sample is re-characterized with two Qubits as the input of QSAN.

**Training** Once the simple dataset is available, QSAN starts randomly assigning initial angles. It then carries out training following the quantum natural gradient training rule instead of the classical gradient descent law [23]. The expectation function is defined as

$$\langle A \rangle = \langle \theta | H | \theta \rangle$$

where the Hamiltonian  $H$  is equal to  $Z_2 Z_3 Z_4 Z_5$  (the subscript here indicates the line number of the quantum circuit), that is, the expectation on the Pauli operator  $Z$  for the observation of lines 2 to 5. The outcomes of quantum natural gradient descent and gradient descent training are shown in Fig. 7. In Fig. 7, the first figure explains the convergence of QSAN during the training process, concluding that the quantum natural gradient descent method converges faster and helps avoid the optimization from falling into local minima. The second figure shows the evolution of the 12 parameter angles during quantum natural gradient descent.

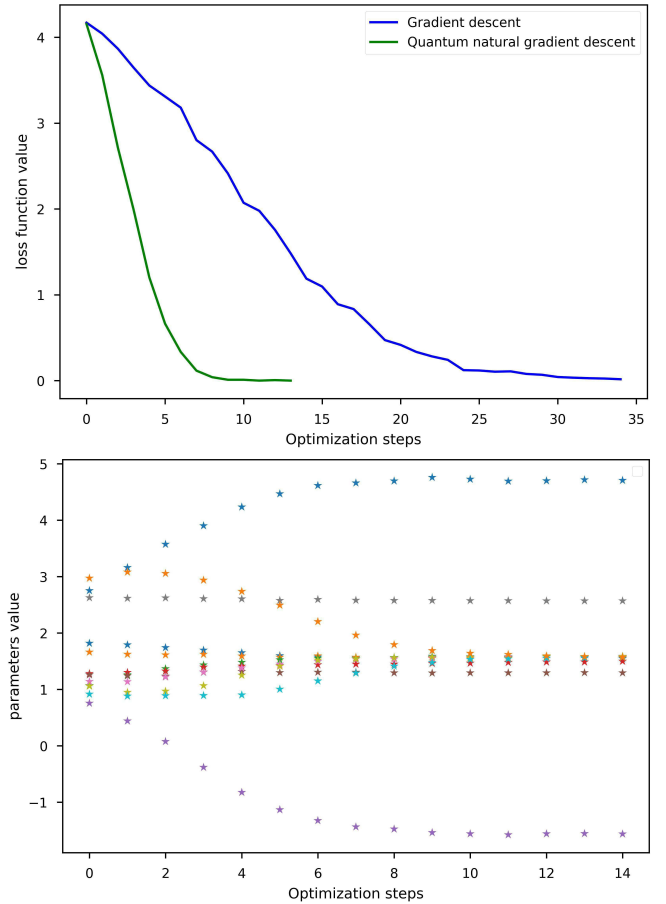


Fig. 7: Training results of QSAN: max\_iterations = 500; conv\_tol = 1e-06; step\_size = 0.115

**QBSASM** Due to the extension of the classical attention score to a quantum state, the QBSASM is thus formed, giving the classical attention score a probabilistic character

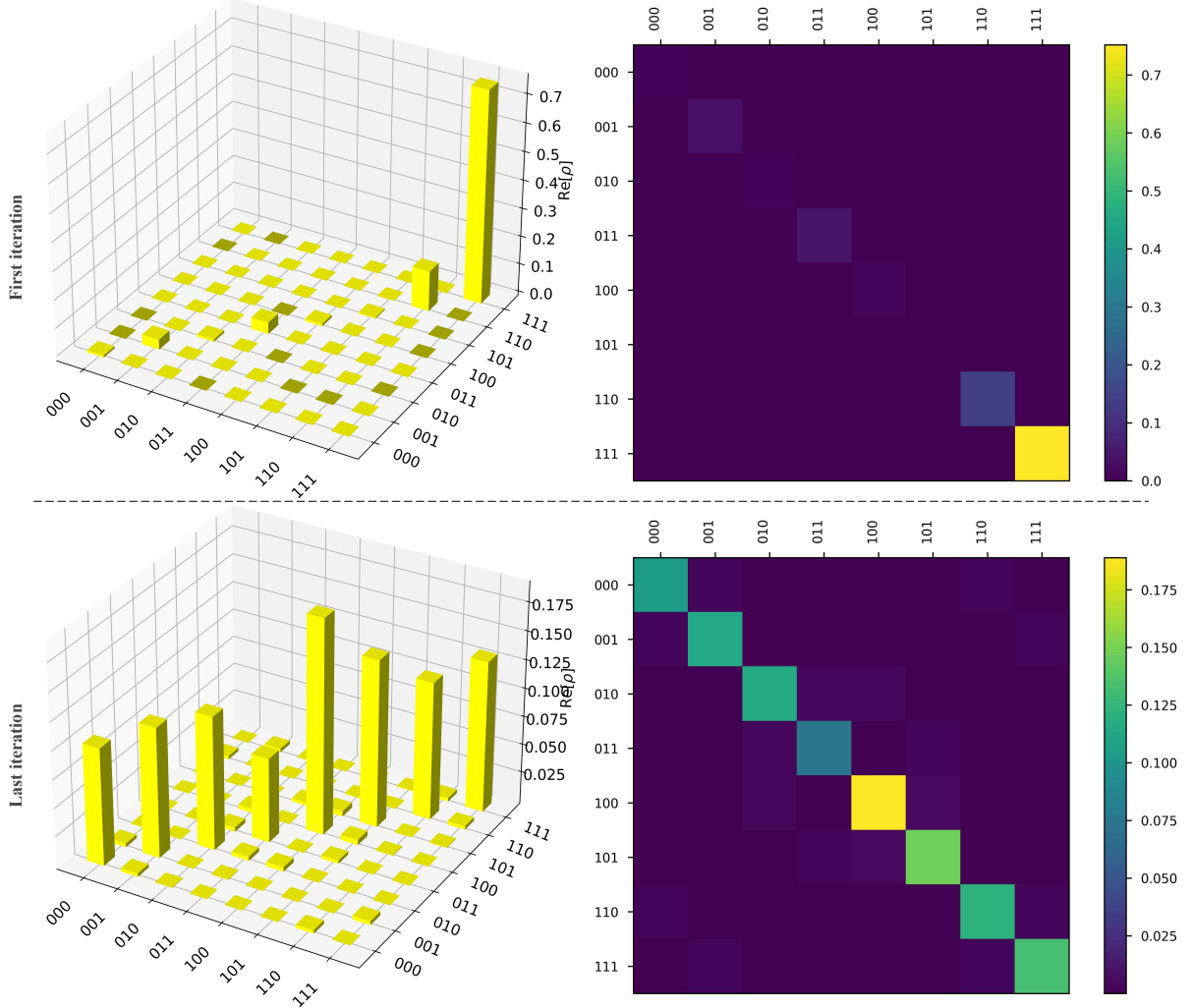


Fig. 8: Quantum attention score matrix

while being higher in dimensionality. At first, the self-attentive fraction presents a random state due to the random assignment of the initialization angle, as shown in the upper part of Fig. 8. After the quantum natural gradient descent, in the last round, a completely new attention distribution is obtained by intercepting this matrix, as in the lower part of Fig. 8. It is worth mentioning that the specific scores need to be known by measurement due to the presence of probabilistic properties, which means that by measurement, the QBSASM also collapses to some specific classical attention score matrix.

**Discussion** QSAN is difficult for ordinary computers to emulate because just one QBSASM consumes a large amount of storage, which is the storage advantage of quantum computers. In addition, QSAN uses logical operations between qubits instead of taking quantum numerical operations, which helps to save the qubits needed to build QSAN.

However, whether more quantum bits can be saved for QSAN is an open question. Quantum coordinates are utilized in the paper, and since it can facilitate the construction of quantum networks with similar structure repetition, whether it will be a subject of further optimization of the structure is worthy of deeper investigation. Establishing a complete

theoretical system of quantum coordinates, and a series of coordinate operations, decomposition, and merging laws may give a more concise form to QSAN.

Further, QSAN, as an important component of machine learning, is merging with machine learning models, such as forming the new Quantum Transformer. whether Quantum Transformer will have a secondary acceleration to the classical model is the next topic of this paper.

## VI. CONCLUSION

In this paper, we propose a QSAN that can be implemented on quantum computers in the near term to lay the foundation for the study of quantum self-attention mechanism. And the theoretical basis of the quantum self-attentive mechanism is explored. The traditional inner product similarity is transformed into logical similarity. In essence, QSAN is a probabilistic linear self-attention mechanism. It has a higher dimensional representation of QBSASM, and it is difficult for general computers to simulate this matrix due to storage limitations. The intercept density matrix allows to observe the QBSASM before and after input on the output distribution.

## ACKNOWLEDGMENT

We would like to thank all the reviewers who provided valuable suggestions.

## REFERENCES

- [1] Ashish Vaswani, Noam Shazeer et al., “Attention is all you need,” in Proceedings of the 31st International Conference on Neural Information Processing Systems, 2017, pp. 6000–6010.
- [2] Tao Shen, Tianyi Zhou et al., “Disan: Directional self-attention network for rnn/cnn-free language understanding,” in Proceedings of the AAAI Conference on Artificial Intelligence, 2018, pp. 5446-5455.
- [3] Naihan Li, Shujie Liu et al., “Neural speech synthesis with transformer network,” in Proceedings of the AAAI Conference on Artificial Intelligence, 2019, pp. 6706-6713.
- [4] J. Fu, J. Liu et al., “Dual attention network for scene segmentation,” in 2019 IEEE/CVF Conference on Computer Vision and Pattern Recognition (CVPR), 2019, pp. 3141-3149.
- [5] Rewon Child, Scott Gray et al., “Generating long sequences with sparse transformers,” arXiv preprint arXiv:1904.10509, 2019.
- [6] S. Zhuoran, Z. Mingyuan et al., “Efficient attention: Attention with linear complexities,” in 2021 IEEE Winter Conference on Applications of Computer Vision (WACV), 2021, pp. 3530-3538.
- [7] Krzysztof Choromanski, Valerii Likhoshesterov et al., “Rethinking attention with performers,” arXiv preprint arXiv:2009.14794, 2020.
- [8] Yunyang Xiong, Zhanpeng Zeng et al., “Nyströmformer: A nyström-based algorithm for approximating self-attention,” in Proceedings of the AAAI Conference on Artificial Intelligence, 2021, pp. 14138-14148.
- [9] Weizhe Hua, Zihang Dai et al., “Transformer quality in linear time,” arXiv preprint arXiv:2202.10447, 2022.
- [10] Frank Arute, Kunal Arya , et al., “Quantum supremacy using a programmable superconducting processor,” Nature, vol. 574, no. 7779, pp. 505-510, 2019.
- [11] Han-Sen Zhong, Hui Wang et al., “Quantum computational advantage using photons,” Science, vol. 370, no. 6523, pp. 1460-1463, 2020.
- [12] Lars S. Madsen, Fabian Laudenbach et al., “Quantum computational advantage with a programmable photonic processor,” Nature, vol. 606, no. 7912, pp. 75-81, 2022.
- [13] Man-Hong Yung, “Quantum supremacy: Some fundamental concepts,” National Science Review, vol. 6, no. 1, pp. 22-23, 2019.
- [14] Aram W. Harrow, and Ashley Montanaro, “Quantum computational supremacy,” Nature, vol. 549, no. 7671, pp. 203-209, 2017.
- [15] R. Di Sipio, J. H. Huang et al., “The dawn of quantum natural language processing,” in ICASSP 2022 - 2022 IEEE International Conference on Acoustics, Speech and Signal Processing (ICASSP), 2022, pp. 8612-8616.
- [16] M. Abbaszade, V. Salari et al., “Application of quantum natural language processing for language translation,” IEEE Access, vol. 9, pp. 130434-130448, 2021.
- [17] John Preskill, “Quantum computing in the nisq era and beyond,” Quantum, vol. 2, pp. 79, 2018.
- [18] Alberto Peruzzo, Jarrod McClean et al., “A variational eigenvalue solver on a photonic quantum processor,” Nature Communications, vol. 5, no. 1, pp. 4213, 2014.
- [19] Marcello Benedetti, Erika Lloyd et al., “Parameterized quantum circuits as machine learning models,” Quantum Science and Technology, vol. 4, no. 4, pp. 043001, 2019.
- [20] Lukasz Cincio, Kenneth Rudinger et al., “Machine learning of noise-resilient quantum circuits,” PRX Quantum, vol. 2, no. 1, pp. 010324, 2021.
- [21] Jonas M Kübler, Andrew Arrasmith et al., “An adaptive optimizer for measurement-frugal variational algorithms,” Quantum, vol. 4, pp. 263, 2020.
- [22] Ryan Sweke, Frederik Wilde et al., “Stochastic gradient descent for hybrid quantum-classical optimization,” Quantum, vol. 4, pp. 314, 2020.
- [23] James Stokes, Josh Izaac et al., “Quantum natural gradient,” Quantum, vol. 4, pp. 269, 2020.
- [24] Abhinav Kandala, Antonio Mezzacapo et al., “Hardware-efficient variational quantum eigensolver for small molecules and quantum magnets,” Nature, vol. 549, no. 7671, pp. 242-246, 2017.
- [25] Nikolay V. Tkachenko, James Sud et al., “Correlation-informed permutation of qubits for reducing ansatz depth in the variational quantum eigensolver,” PRX Quantum, vol. 2, no. 2, pp. 020337, 2021.
- [26] E. Farhi, J. Goldstone et al., “A quantum approximate optimization algorithm,” arXiv: Quantum Physics, 2014.
- [27] Stuart Hadfield, Zhihui Wang et al., “From the quantum approximate optimization algorithm to a quantum alternating operator ansatz,” Algorithms, vol. 12, no. 2, 2019.
- [28] M. E. S. Morales, J. D. Biamonte et al., “On the universality of the quantum approximate optimization algorithm,” Quantum Information Processing, vol. 19, no. 9, pp. 291, 2020.
- [29] Harry Buhrman, Richard Cleve et al., “Quantum fingerprinting,” Physical Review Letters, vol. 87, no. 16, pp. 167902, 2001.
- [30] Dorit Aharonov, Vaughan Jones et al., “A polynomial quantum algorithm for approximating the jones polynomial,” Algorithmica, vol. 55, no. 3, pp. 395-421, 2009.
- [31] Carlos Ortiz Marrero, Mária Kieferová et al., “Entanglement-induced barren plateaus,” PRX Quantum, vol. 2, no. 4, pp. 040316, 2021.
- [32] Jarrod R. McClean, Sergio Boixo et al., “Barren plateaus in quantum neural network training landscapes,” Nature Communications, vol. 9, no. 1, pp. 4812, 2018.
- [33] Qiskit Development Team. ”Realamplitudes documentation,” <https://qiskit.org/documentation/stubs/qiskit.circuit.library.RealAmplitudes.html>.

This figure "thumbnail.jpeg" is available in "jpeg" format from:

<http://arxiv.org/ps/2207.07563v1>